Journal of Science Research and Reviews

PRINT ISSN: 1595-9074
E-ISSN: 1595-8329
DOI: https://doi.org/10.70882/josrar.2025.v2i5.120
Homepage: https://josrar.esrgngr.org

Original Research Article

Effect of a Spring-Bocked Membrane on a Falling Film over a Slippery Tilted Plane

[1]Suleiman Abbey Bello, *[1]Muhammad Sani, [2]Iliyasu Bello, [1]Bamanga Ibn Dawuda, [1]Kabiru Garba Ibrahim, [1]Naziru Nura, [1]Oladele Yusuf Olatunji and [1]Mamuda Alhaji Mamuda

[1]Federal University Dutse, Faculty of Physical Sciences, Department of Mathematics, Dutse, Jigawa, Nigeria.
[2]Modibbo Adama University of Technology, Yola, faculty of Sciences Department of Mathematics, Yola, Adamawa.
*Corresponding Author's email: msdjunior9@gmail.com

KEYWORDS

Stability analysis,
Spring-bocked membrane,
Film flow,
Slippery plane,
Reynolds number,
Orr-Sommerfeld analysis,
Wave number,
Spectral method,
Free Surface instabilities.

CITATION

Bello, S. A., Sani, M., Bello, I., Dawuda, B. I., Ibrahim, K. G., Nura, N., Olatunji, O. Y., & Mamuda, M. A. (2025). Effect of a Spring-Bocked Membrane on a Falling Film over a Slippery Tilted Plane. *Journal of Science Research and Reviews*, *2*(5), 49-56. https://doi.org/10.70882/josrar.2025.v2i5.120

ABSTRACT

This research work investigates the influence of a spring-blocked membrane on a perturbed gravity-driven viscous fluid flow down a slippery inclined plane. The spring-bocked membrane on a falling film flow over a slippery plane can affect the flow dynamics and stability of the film. The instability of such a flow can be controlled either by modifying the behavior of the lower wall, altering the surface waves at the free surface using structures, or both, as done here by incorporating a spring-backed membrane at the top of the liquid layer and a slippery substrate. A linear stability analysis is performed utilizing the normal mode approach, with the free surface modified by a spring-blocked membrane and the lower boundary modeled as a slippery substrate. The associated Orr-Sommerfeld system is solved numerically using the spectral collocation method. The results reveal that velocity slip at the lower wall has a non-trivial impact on flow stability: it destabilizes at the onset of instability, then stabilizes at higher Reynolds numbers. Membrane tension is modeled as a stress jump at the free surface, and the mass of the membrane is also taken into account. The findings demonstrate that increasing the dimensionless spring-blocked membrane tension (T) reduces the growth rate of the most unstable mode, thereby enhancing flow stability. Thus, combination of a spring-blocked membrane at the free surface and a slippery base exerts a significant passive control on flow stability. The study provides an insight into how such configurations can be utilized to either suppress or amplify interfacial instabilities in gravity-driven flows.

INTRODUCTION

Hydrodynamic stability analysis and transition behavior has a vast applications in biomedical, industries and agricultural engineering (Criminale *et al*., 2003, Vallentine 2013, Newman 2018, etc.). Free-surface fluid flow along inclined or vertical planes has attracted and continues to attract the attention of significant number of researchers (Oron *et al.*, 1997, Chang and Demekhin 2002, Thiele et al., 2012 O'Connor and Benedict 2021, etc.) due to its complex spatiotemporal patterns, which are relevant to processes such as film cooling and coating. Surface tension plays a key role in governing wave characteristics in fluid flows. Instability in a single-layer falling film over an inclined wall primarily arises from inertial effects, while interfacial instabilities are driven by kinetic mechanisms (Kao 1965, Kao 1968, Sani *et al.*, 2020, etc.). A landmark contribution to this field is Yih's work (1963) on the stability of film flow down an inclined plane. Chin and Bertschy (1986) demonstrated that variations in surface tension can destabilize gravity-driven flow at low to moderate Reynolds numbers by inducing an unstable surface mode. To control such instabilities, several strategies using surface-active or inactive agents have been proposed (Li and Pozrikidis 1997, Blyth and Pozrikidis 2004, Anjalaiah *et al.,* 2013). Numerous studies have since explored methods for stabilizing or destabilizing surface waves in laminar single-layer flows of Newtonian and non-Newtonian fluids over inclined planes (Yih 1963, Liu and Liu 2009, Sani *et al.,* 2020, Subham and Samanta 2021, Choudhury and Samanta 2022, etc.). Benjamin *et al*., (1957) theoretically investigated the hydrodynamic stability of a viscous, laminar liquid film flowing down an inclined plane at low Reynolds numbers, bounded by a free surface influenced by surface tension. Samanta *et al.,* (2011) analyzed flow down a vibrating inclined plane and showed that at higher inclination angles, surface-wave stability is not guaranteed, and the flow remains unsteady. Dholey and Gorai (2021) studied surface-wave instability in a similar configuration, establishing the stability criterion and identifying the critical wave number that suppresses inertial effects.

Several researchers have explored the physical mechanisms behind free-surface flow instabilities and proposed both active and passive strategies to control them in single- and multi-layer films (Sani *et al.,* 2021, Li *et al.*, 2023 Samanta 2025, etc.). One standard control method involves applying an insoluble surfactant at the free surface, which acts as a surface-active agent to influence flow stability (Samanta 2025). Thiele *et al.,* (2012) developed a thermodynamically consistent model for free surfaces covered with high concentrations of insoluble surfactants and reviewed the classical evolution equations for film height and surfactant distribution. Blyth and Pozrikidis (2004) examined the stabilizing influence of surfactants on the Yih mode, showing that variations in surface tension induced by surfactants generate an additional instability mechanism, the Marangoni mode.

Applying external shear at the free surface is another active method for controlling surface-wave energy, with practical relevance in processes such as airway blockage (Otis *et al.,* 1993). Samanta (2014) and Sani *et al.,* (2020) examined the effect of external shear on gravity-driven falling films over a steep, rigid incline and showed that an externally applied force enhances long-wave instability by reducing the critical Reynolds number. Later, Bhat and Samanta (2018) investigated the influence of external shear on a surfactant-covered film and demonstrated that insoluble surfactants can reduce the wave energy generated by the external force. Another approach to controlling instability in gravity-driven film flows is to modify the behavior of the lower wall or substrate. This method is theoretically important and has significant industrial relevance (Wang 1984, Pascal 1999, Pascal 2006, Das *et al.,* 2024, etc.). Many natural and engineering processes, such as surface water movement, soil transport, and groundwater flow through cracks, can be modeled as thin-film flow over a porous inclined wall. In such studies, the effect of wall porosity on flow dynamics and stability is examined, with Darcy's law governing the flow within the porous medium (Pascal 1999, and Pascal 2006). Film that flows over porous substrates have been shown to exhibit enhanced stability, as the porous structure dissipates energy and suppresses disturbances (Anjalaiah *et al*., 2004, Sani *et al.,* 2021, Samanta 2023, etc.). Notably, Pascal (2006) demonstrated that increasing the permeability of the porous substrate reduces instability in a Newtonian thin film, highlighting the stabilizing influence of porous walls. Liu and Liu (2009) investigated shear-driven film flow down an inclined porous plane. At the same time, Pascal and D'Alessio (2010) developed a theoretical model accounting for fluid porous medium interaction and showed that low permeability destabilizes the film. Usha *et al*., (2011) modeled flow over a weakly porous bottom for a tension-thinning film, incorporating filtration effects and porous-layer influence at the interface. Kandel and Pascal (2013) analyzed interfacial instability of film flow down porous inclines at low to moderate Reynolds numbers and reported conditions leading to instability. Anjalaiah *et al*., (2013) studied thin-film flow over a porous bed with surfactant and found that increasing permeability lowers the critical Reynolds number and enlarges the range of unstable wave numbers, for both clean and surfactant-covered films.

Beyond porous substrates, instability in film flow can also be controlled by introducing slip at the lower wall. Several mathematical and experimental studies have examined the transition between slippery and no-slip behaviour in gravity-driven films on inclined surfaces (Samanta *et al.,* 2011, Samaha and Hak 2021, Tripathi *et al*., 2023). Samanta *et al.,* (2011) analysed film flow down a slippery inclined plane and demonstrated that slip length significantly affects wave evolution in both linear and nonlinear regimes. Their results show that applying the Navier slip condition enhances back-flow in the capillary region of solitary waves and can influence heat and mass transfer. Their study extends Benney's long-wave expansion theory (Benney 1996) to moderate Reynolds numbers by relaxing the restrictions on free-surface velocity development. Ding and Wong (2015) examined liquid-film flow over a uniformly slippery substrate and showed that the combination of wall slip and inertia increases both phase speed and wave amplitude. Bhat and Samanta (2018) performed a linear stability analysis on film flow over a slippery inclined plane. They extended the findings of Samanta *et al*., (2011), demonstrating that wall slip stabilizes the surface mode at moderate Reynolds numbers, a behavior different from that observed in the long-wave regime. Ma *et al.,* (2020) studied the influence of wall slippage on the instability of gravity-driven film flow. They found that, in thin films with moving contact lines, slip in the streamwise and spanwise directions has opposite effects. However, slip in either direction can still destabilize under dynamic contact-line conditions.

To the best of the authors' knowledge, no previous study has examined film flow down a slippery inclined plane in the presence of a spring-backed membrane at the free surface. This work addresses that gap by performing a linear stability analysis of gravity-driven film flow with a slippery substrate and a spring-backed membrane. The membrane boundary conditions follow Karmakar and Sahoo (2008). Using normal-mode analysis, the Orr Sommerfeld equations are formulated and solved via a spectral collocation method in a two-dimensional Cartesian framework. The effects of membrane tension, inclination angle, and slip length are examined. The results show that membrane tension destabilizes over a wide range of parameters and, when combined with wall slip, increases the growth rate of perturbation waves. The study provides a systematic derivation of the governing equations and presents numerical results demonstrating the interplay between the membrane and slippery substrate in controlling flow stability.

MATERIALS AND METHODS

Mathematical Formulation

A two-dimensional, incompressible Newtonian fluid flowing over a slippery inclined plane is considered. The interaction between the fluid surface and a spring-backed membrane is analyzed in a Cartesian coordinate system, where the (x) −axis lies along the inclined slippery plane and the (y) −axis is oriented vertically upward from the plane (Fig.1). The membrane is assumed to have uniform thickness and rests on the free surface of the fluid layer at $(y = d)$, where its displacement is denoted by $\left(y = \eta(x,t)\right)$. The mean fluid surface is parallel to the inclined plane and corresponds to $(y = 0)$.

$$\frac{\partial u}{\partial x} + \frac{\partial v}{\partial y} = 0, \tag{1}$$

$$\rho\left(\frac{\partial u}{\partial t} + u\frac{\partial u}{dx} + v\frac{\partial u}{\partial y}\right) = -\frac{\partial p}{\partial x} + \mu\left(\frac{\partial^2 u}{\partial x^2} + \frac{\partial^2 u}{\partial y^2}\right) + g\rho sin\theta, \tag{2}$$

$$\rho\left(\frac{\partial v}{\partial t} + u\frac{\partial v}{dx} + v\frac{\partial v}{\partial y}\right) = -\frac{\partial p}{\partial y} + \mu\left(\frac{\partial^2 v}{\partial x^2} + \frac{\partial^2 v}{\partial y^2}\right) + g\rho cos\theta, \tag{3}$$

where ρ and μ denotes the density and viscosity of the fluid respectively. u and v are the components of velocity in the x and y increasing directions respectively and p is the dynamic pressure exerted by the fluid on the spring-bocked membrane. The term g represents the acceleration due to gravity and θ is the angle of inclination of the substrate.

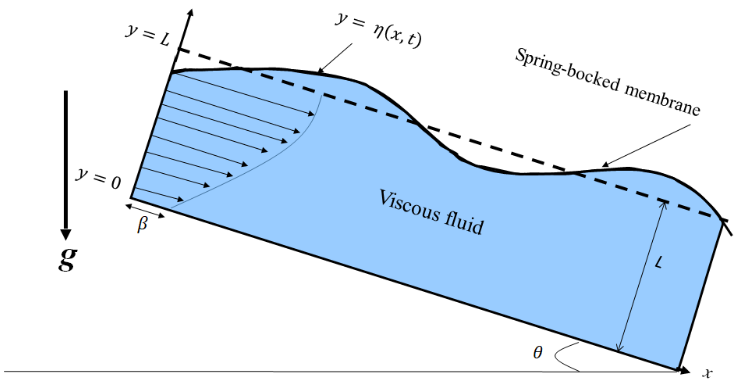

Figure 1: Schematic diagram for a single-layer thin film flow down an inclined slippery wall with a spring-bocked membrane at the free surface

The set of dimensional boundary conditions at the free surface $\left(y = \eta(x,t)\right)$ which is associated with the spring-bocked membrane are the kinematic condition, the balance of the normal and tangential stresses respectively given by

$$v = \frac{\partial \eta}{\partial t} + u\frac{\partial \eta}{\partial x} \quad \text{at } y = \eta(x,t), \tag{4}$$

$$\mu\left[\left(\frac{\partial u}{\partial z} + \frac{\partial v}{\partial x}\right)\left(1 - \left(\frac{\partial \eta}{\partial x}\right)^2\right) - 4\frac{\partial u}{\partial x}\frac{\partial \eta}{\partial y}\right] = 0 \quad \text{at } y = \eta(x,t), \tag{5}$$

$$p - p_\infty = \frac{2\mu}{\left(1+\left(\frac{\partial \eta}{\partial x}\right)^2\right)}\left[\frac{\partial u}{\partial x}\left(\frac{\partial \eta}{\partial x}\right)^2 - \left(\frac{\partial u}{\partial y} + \frac{\partial v}{\partial x}\right)\frac{\partial \eta}{\partial x} + \frac{\partial v}{\partial y}\right] - \frac{T\frac{\partial^2 \eta}{\partial x}}{\left(1-\left(\frac{\partial \eta}{\partial x}\right)^2\right)^{\frac{3}{2}}} - m_m\frac{\partial^2 \eta}{\partial t^2} + T\eta, \text{at } y = \eta(x,t), \tag{6}$$

where T is the membrane tension per length, p_∞ is the atmospheric pressure, and m_m is the uniform mass per unit length of the membrane. Note that, when the elastic membrane is stretched with a constant tension per unit length (i.e. $T = cons$) then $T_x = 0$ and therefore, the right-hand side of the equation (5) will be zero. The boundary conditions at the slippery inclined wall are given as

$$u = \beta\frac{\partial u}{\partial y} \quad \text{at } y = 0, \tag{7}$$

$$v = 0 \quad \text{at } y = 0, \tag{8}$$

where β is the slip length parameter, which confirms the velocity slip at the wall, which enhances the basic flow rate. The set of equations and boundary conditions is made non-dimensional using the following dimensionless variables:

$\bar{x} = \frac{x}{L},\ \ \bar{y} = \frac{y}{L},\ \ \bar{u} = \frac{u}{V},\ \ \bar{v} = \frac{v}{V},\ \ \bar{t} = \frac{tV}{L},\ \ \bar{p} = \frac{p}{\rho V^2},\ \ \bar{\eta} = \frac{\eta}{L}, \bar{T} = \frac{2T}{\rho g sin(\theta) L^2},$

where d is the mean film thickness of the fluid layer and T_0 is the mean reference tension of the spring-bocked membrane. The characteristic velocity scale V for the fluid layer is chosen as the maximum velocity of a uniform flat Nusselt film over a rigid substrate, and given by $\frac{gL^2 sin\theta}{2v}$ and $v = \frac{\mu}{\rho}$ is the kinematic viscosity. The present study is motivated by the investigations by Blyth and Pozrikidis (2004), Sani *et al.,* (2018), and hence, in order to compare the results with available results, the formulation is in terms of the Reynolds number based on the Nusselt film free surface velocity for a film without membrane over a rigid substrate has been used. After suppressing the bars, the set of dimensionless governing equations for the flow beneath the membrane and the set of boundary conditions associated with the membrane are as follows respectively,

$$\frac{\partial u}{dx} + \frac{\partial v}{\partial y} = 0, \quad (9)$$

$$\frac{\partial u}{dt} + u\frac{\partial u}{\partial x} + v\frac{\partial u}{\partial y} = -\frac{\partial p}{\partial x} + \frac{1}{Re}\left[\frac{\partial^2 u}{\partial x^2} + \frac{\partial^2 u}{\partial y^2}\right] + N, \quad (10)$$

$$\frac{\partial v}{\partial t} + u\frac{\partial v}{\partial x} + v\frac{\partial v}{\partial y} = -\frac{\partial p}{\partial y} + \frac{1}{Re}\left[\frac{\partial^2 v}{\partial x^2} + \frac{\partial^2 v}{\partial y^2}\right] - Ncot\theta, \quad (11)$$

$$v = \frac{\partial \eta}{\partial t} + u\frac{\partial \eta}{\partial x} \quad \text{at } y = \eta(x,t), \quad (12)$$

$$\left(1 - \left(\frac{\partial \eta}{\partial x}\right)^2\right)\left(\frac{\partial u}{\partial y} + \frac{\partial v}{\partial x}\right) - 4\frac{\partial u}{\partial x}\frac{\partial \eta}{\partial x} = 0 \quad \text{at } y = \eta(x,t), \quad (13)$$

$$p = \frac{2}{Re\left(1+\left(\frac{\partial \eta}{\partial x}\right)^2\right)}\left[\frac{\partial u}{\partial x}\left(\frac{\partial \eta}{\partial x}\right)^2 - \left(\frac{\partial u}{\partial y} + \frac{\partial v}{\partial x}\right)\frac{\partial \eta}{\partial x} + \frac{\partial v}{\partial x}\right] - \frac{gLsin(\theta)T\frac{\partial^2 \eta}{\partial x^2}}{2v^2\left(1+\left(\frac{\partial \eta}{\partial x}\right)^2\right)^{\frac{3}{2}}} - \frac{m_m}{\rho vL}\frac{\partial^2 \eta}{\partial t^2} + \frac{T(\eta+1)}{\rho v^2} \quad \text{at } y = \eta(x,t), \quad (14)$$

$$u = \frac{\beta}{L}\frac{\partial u}{\partial y} \quad \text{at } y = 0, \quad (15)$$

$$v = 0 \quad \text{at } y = 0, \quad (16)$$

in the above equations, $N = \frac{Lgsin\theta}{V^2}$ is the modified Galileo number, $Re = \frac{VL}{v}$ is called the Reynolds number of the flow, and remark that T and m_m are the dimensionless membrane tension and unit mass.

Base solution and stability equations

The base flow solution corresponding to the flow below the spring-bocked membrane obtained from the corresponding set of equations above and boundary conditions is respectively given by

$$U(y) = y(2-y) + 2\beta, \quad (17)$$

$$P(y) = 2cot\theta(1-y). \quad (18)$$

Where $0 \leq \beta \leq 1$, utilizing the research of Anjalaiah *et al.,* (2013), the base flow calculation is done by setting $N\,Re = 2\,(N \simeq O(1))$. It is important to note that there will be no change in the behaviors of the base flow due to the presence of the membrane at the free surface.

Next, the stability of the base state with respect to infinitesimal perturbations is considered, and the flow variables are now taken as the sum of the basic state and the perturbed state solution. Substituting $u(x,y,t) = U(y) + \tilde{u}(x,y,t)$, $v(x,y,t) = \tilde{v}(x,y,t)$, $p(x,y,t) = P(y) + \tilde{p}(x,y,t)$ and $\eta(x,t) = 1 + \tilde{\eta}(x,t)$ into the equations of motion and boundary conditions, and linearizing with respect to the small amplitude perturbations, the equations for the perturbed quantities are obtained as

$$\frac{\partial \tilde{u}}{\partial \tilde{x}} + \frac{\partial \tilde{v}}{\partial \tilde{y}} = 0, \quad (19)$$

$$Re\left(\frac{\partial \tilde{u}}{\partial \tilde{t}} + U\frac{\partial \tilde{u}}{\partial \tilde{x}} + \tilde{v}\frac{\partial U}{\partial \tilde{y}}\right) = -Re\frac{\partial \tilde{p}}{\partial \tilde{x}} + \left(\frac{\partial^2 \tilde{u}}{\partial \tilde{x}^2} + \frac{\partial^2 \tilde{u}}{\partial y^2}\right), \quad (20)$$

$$Re\left(\frac{\partial v}{\partial \tilde{t}} + U\frac{\partial \tilde{v}}{\partial \tilde{x}}\right) = -Re\frac{\partial \tilde{p}}{\partial \tilde{y}} + \left(\frac{\partial^2 \tilde{v}}{\partial \tilde{x}^2} + \frac{\partial^2 \tilde{v}}{\partial y^2}\right), \quad (21)$$

$$\tilde{v} = \frac{\partial \tilde{\eta}}{\partial \tilde{t}} + U\frac{\partial \tilde{\eta}}{\partial \tilde{x}} \quad \text{at } y = 1, \quad (22)$$

$$\left(\frac{\partial \tilde{u}}{\partial \tilde{y}} + \frac{\partial \tilde{v}}{\partial \tilde{x}} + \frac{\partial U}{\partial \tilde{y}}\right)\left(1 - \left(\frac{\partial \tilde{\eta}}{\partial \tilde{x}}\right)^2\right) = 0 \quad \text{at } y = 1, \quad (23)$$

$$P(y) + \tilde{p} = \frac{2}{Re\left(1+\left(\frac{\partial \eta}{\partial x}\right)^2\right)}\left(\frac{\partial \tilde{v}}{\partial \tilde{y}} - \frac{\partial U}{\partial \tilde{y}}\frac{\partial^2 \tilde{\eta}}{\partial \tilde{y}}\right) - \frac{\frac{Lgsin\theta}{2V^2}T\frac{\partial \tilde{\eta}}{\partial \tilde{x}^2}}{\left(1+\left(\frac{\partial \eta}{\partial x}\right)^2\right)^{\frac{3}{2}}} - \frac{m_m}{\rho vd}\frac{\partial^2 \tilde{\eta}}{\partial \tilde{t}^2} + \frac{T(1+\eta)}{\rho v^2} \quad \text{at } \tilde{y} = 1 \quad (24)$$

Using Eq. (19) in Eq. (24), and linearizing Eq. (23), one can rewrite these equations after simplifying as,

$$\frac{\partial^2 \tilde{u}}{\partial \tilde{y}\partial \tilde{x}} + \frac{\partial^2 \tilde{v}}{\partial \tilde{x}^2} = 0 \quad \text{at y} = 1, \quad (25)$$

$$Re^{-1}\left(\frac{\partial^3 \tilde{u}}{\partial \tilde{x}^3} + \frac{\partial^3 \tilde{u}}{\partial \tilde{x}\partial y^2}\right) - \left(\frac{\partial^2 \tilde{u}}{\partial \tilde{t}\partial \tilde{x}} + \frac{U\partial^2 \tilde{u}}{\partial \tilde{x}^2} + \frac{\partial \tilde{v}}{\partial \tilde{x}}\frac{\partial U}{\partial \tilde{y}}\right) = \frac{2}{Re}\left(\frac{\partial^3 \tilde{v}}{\partial \tilde{y}\partial \tilde{x}^2} - U\frac{\partial^2 \tilde{\eta}}{\partial \tilde{x}^3}\right) - \frac{Lgsin\theta}{2v^2}T\frac{\partial^4 \tilde{\eta}}{\partial \tilde{x}^4} - \frac{m_m}{\rho vd}\frac{\partial^4 \tilde{\eta}}{\partial \tilde{t}^2\partial \tilde{x}^2} + \frac{T}{\rho v^2}\frac{\partial^2 \tilde{\eta}}{\partial \tilde{x}^2} \quad \text{at } y = 1, \quad (26)$$

$$\frac{\partial \tilde{u}}{\partial \tilde{x}} = \frac{\beta}{d}\frac{\partial^2 \tilde{\eta}}{\partial \tilde{x}^2} \quad \text{at } y = 1, \quad (27)$$

$$\tilde{v} = 0 \quad \text{at } y = 0. \quad (28)$$

Let $\tilde{\psi}$ be the stream function of the dimensional flow below the spring-bocked membrane, in the form of normal mode solution, $\tilde{\psi}(x,y,t) = \phi(y)e^{i\alpha(x-ct)}$ and $\tilde{\eta}(x,y,t) = \Omega(y)e^{i\alpha(x-ct)}$, where α and c are the wave number and the complex wave speed, respectively, and $i \equiv \sqrt{-1}$. Expressing the velocity components in terms of stream function and using all in the linearized perturbed equations and boundary conditions, the following Orr-Sommerfeld system is obtained,

$$(c-U)D^2\theta - (c-1)\alpha^2 D^0 + \frac{\partial^2 U}{\partial \tilde{z}^2}D^0\phi = -i(\alpha Re)^{-1}(\alpha^4 D^0\phi - 2\alpha^2 D^2\phi + D^4\emptyset), \quad (29)$$

$$D^0\phi + \Omega(U-c) = 0 \quad at\ y = 1, \quad (30)$$

$$D^2\phi + \alpha^2 D^0\phi = 0 \quad at\ y = 1, \quad (31)$$

$$iRe^{-1}(D^3\phi + \alpha^2 D\phi) - \left(\alpha cD\phi - \alpha UD\phi + \alpha i\frac{\partial U}{\partial \tilde{z}}D^0\phi\right) = \frac{2i\alpha^3}{Re}\left[D\phi + \frac{\partial U}{\partial \tilde{z}}\Omega\right] - \frac{dgsim(\theta)}{2v^2}T\alpha^4\Omega - \frac{m_m\alpha^4}{\rho vd}c^2\Omega - \frac{T\alpha^2\Omega}{\rho v^2} \quad at\ y = 1, \quad (32)$$

$$D\phi = \frac{\beta}{d}D^2\phi \quad \text{at y} = 0, \quad (33)$$

$$D^0\phi = 0 \quad \text{at } y = 0, \quad (34)$$

where D denotes derivative with respect to y. Equations (29)−(34) describe a generalized eigenvalue problem with c as an eigenvalue, and we are interested in obtaining a non-trivial solution of the system. The parameter $c = c_r + ic_i$ where c_r and c_i are respectively, the wave speed and the growth rate. However, when there is no spring-bocked membrane present at the free surface and no slippage at the substrate, the above system reduces to the Orr-Sommerfeld equations representing a Newtonian flow down a rigid inclined substrate given by Yih (1963). On the other hand, when we consider the spring-bocked membrane at the free surface, then the Orr-Sommerfeld equations obtained resemble those which were obtained by Blyth and Pozrikidis (2004).

RESULTS AND DISCUSSION

The Orr–Sommerfeld model is solved using the spectral collocation method following Canuto *et al.,* (2012), where Chebyshev polynomials and Chebyshev collocation points are used to discretize the generalized eigenvalue problem given in Eqs. (29)–(32). Solving this eigenvalue system yields the complex phase velocity $c = c_r + ic_i$, from which the dimensionless growth rate is obtained as $\omega_i = \alpha c_i$for a wide range of wave numbers α. The accuracy of the computed eigenvalues is verified by increasing the number of collocation points, and any spurious eigenvalues are removed through a filtering procedure.

The MATLAB code used for the computation is validated by comparing the growth-rate results for a film flow over a rigid inclined surface without the membrane. The numerical results show excellent agreement with previously published studies. Subsequently, the influence of membrane mass m_m, spring-backed membrane tension T, slip parameter β, and Reynolds number Reon flow stability is examined. The analysis also includes the effects of parameters associated with both the membrane and the slippery substrate Results reveal that introducing a floating membrane on the free surface generally enhances the stability of an otherwise unstable flow. Increasing the membrane mass m_m further stabilizes the flow, as indicated by the decreasing growth rate (see dashed curves in Fig. 2). The thin membrane responds to perturbations and generates additional surface waves. These membrane-induced

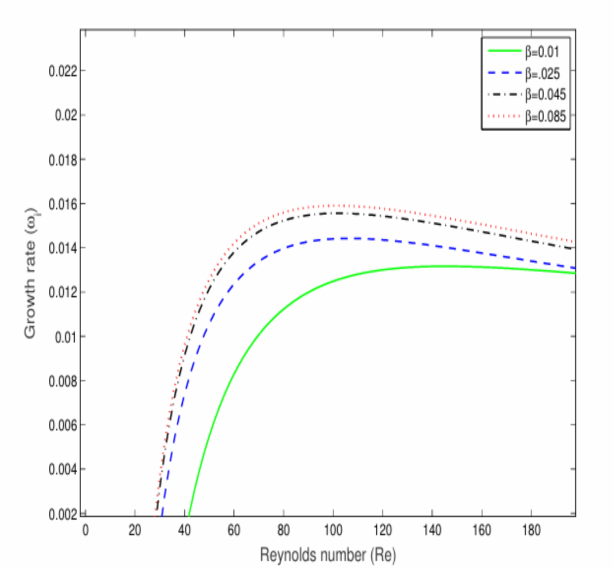

Figure 2: The growth rate of the dominant mode as a function of Reynolds number for different values of Beta (β) when $k = 0.2, \theta = 4^o, T = 0.01$, and membrane mass $m_m = 0.01$

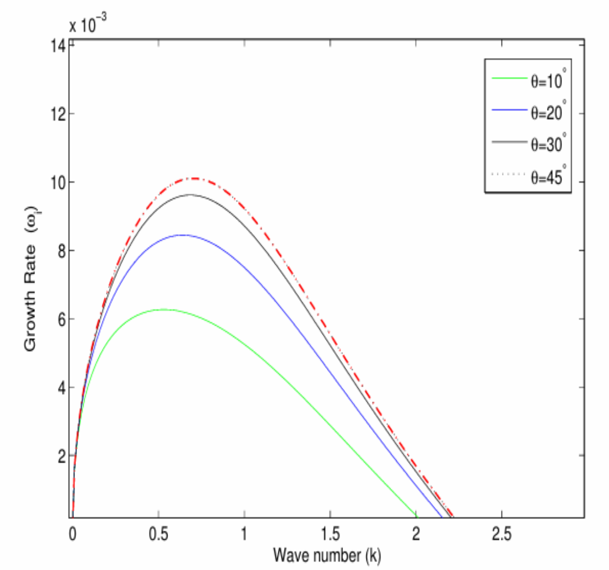

Figure 3: The growth rate of the dominant mode as a function of wave number for different values of angle of inclination (θ) when $Re = 1500, T = 0.01, \beta = 0.001$ and $m_m = 0.01$

Figure 2 shows the results for the growth rate as a function of wave number for different values of Beta (β). The results reveal that for $\beta = 0.01$ (represented in Figure 5 by the solid curves), The growth rate of the most unstable mode is higher compared to the other values of β Considered (shown by the dashed curves). It is also observed that when the wave number reaches 0.025, the growth rate begins to decline for all values of β. These observations are similar to that observed by Khan *et al.,* (2021) for slippery substrate. Therefore, the system's instability increases with the slip parameter. This illustrates the influence of β on the system. Figure 3 shows the growth rate of the dominant mode as a function of wave number for different inclination angles θ. For $\theta = 45°$(solid curve), the maximum growth rate is the smallest compared to the other angles (dashed curves). In all cases, the growth rate increases with wave number, reaches a peak, and then decreases. This demonstrates that the inclination angle influences flow stability. These observations are similar to that made by Sani *et al.*, (2018). As θincreases, the maximum growth rate of the most unstable mode also increases, indicating reduced stability at higher inclination angles.

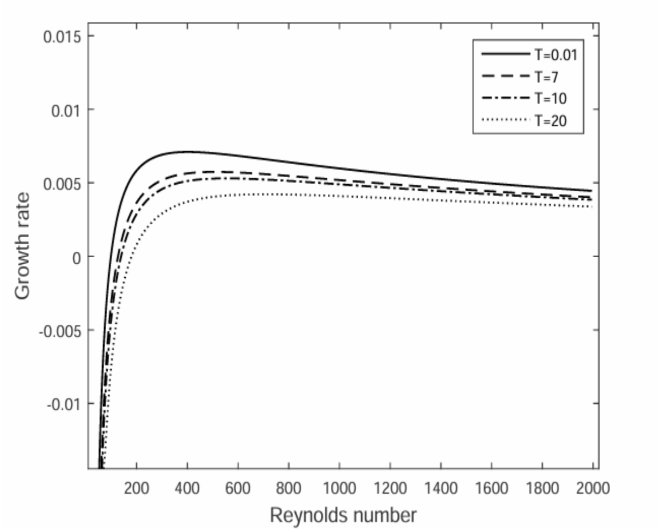

Figure 4: The growth rate of the dominant mode as a function of Reynolds number for different values of membrane tension when $\theta = 4^o, \beta = 0.001, k = 0.2$ and membrane mass $(m_m) = 0.01$.

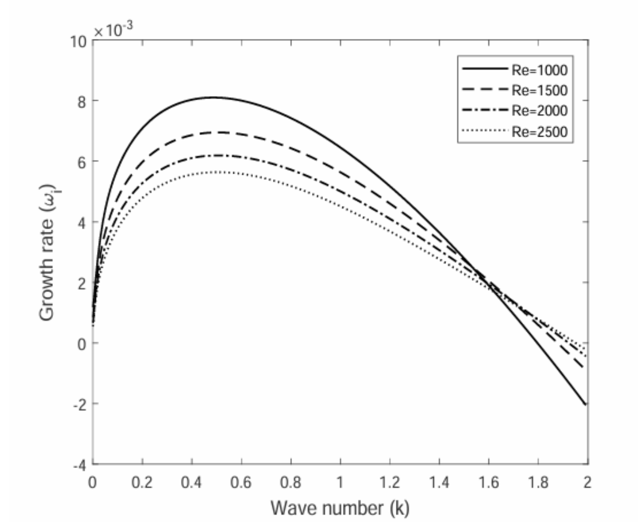

Figure 5: The growth rate of the dominant mode as a function of wave number for different values of Reynolds number (*Re*) when $\theta = 4^o, T = 0.01, \beta = 0.001, k = 0.2$ and membrane mass $m_m = 0.01$

Figure 4 presents the growth rate of the dominant mode as a function of Reynolds number (Re) for different membrane tensions (T). Increasing Treduces the growth rate of the unstable mode, thereby enhancing flow stability. For all values of T, the growth rate increases with Re, eventually crossing zero and becoming unstable. Since membrane tension introduces a stress jump at the free surface, higher tension suppresses instability. A related study was conducted and similar result was obtained by Sani *et al.*, (2020). Thus, the flow remains more stable at lower Re, and increasing membrane tension enhances overall flow stability. Figure 5 illustrates the effect of the Reynolds number (Re) on the growth rate of the dominant mode as a function of wave number. When $Re = 1500$ (solid curve), the maximum growth rate is highest compared to the lower Re Values (dashed curves). For all cases, the growth rate initially increases with wave number, reaches a peak, and then declines. Its observed that a bifurcation occurs around $k \approx 0.2$. This indicates that higher Re enhances flow instability, while lower Re values promote greater flow stability. A related study was conducted and similar result was obtained by Sani et al., (2018) regarding the floating membrane at the free surface.

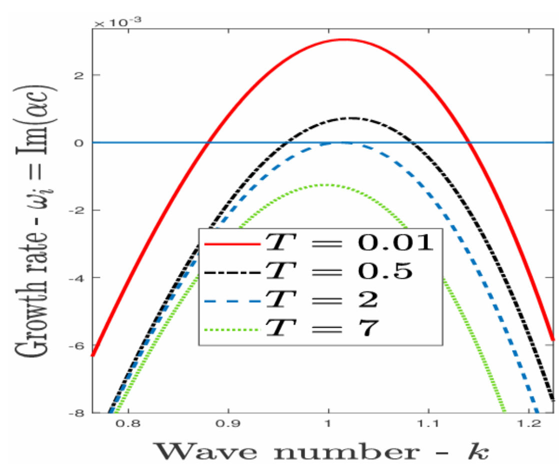

Figure 6: The growth rate of the dominant mode as a function of wave number for different values of membrane tension when $Re = 1500$, $\theta = 4^o$, $\beta = 0.001$ and membrane mass $m_m = 0.01$.

Figure 6 shows the variation of the growth rate with respect to wave number for different membrane tension (T). As membrane tension (T) As membrane tension increases, it introduces a larger stress jump at the free surface, thereby influencing flow stability. The growth rate increases with wave number, reaches a maximum, and then decreases. A related study was conducted and similar result was obtained by Sani et al., (2018) regarding the floating membrane at the free surface. While the baseline flow (without the membrane) exhibits a higher peak growth rate, increasing membrane tension reduces the maximum growth rate of the most unstable mode. Thus, greater membrane tension enhances flow stability.

CONCLUSION

This study has observed the impact of a spring-blocked membrane and a slippery inclined substrate on a perturbed gravity-driven viscous fluid flow. Using the spectral collocation method, the research has depicts that the spring-bocked plays a vital role in controlling the instability of the system. Increase in the membrane tension causes more energy deflection at the free surface. Thus, the study found that membrane tension generally contributes in enhancing the fluid flow instabilities. Furthermore, the spring-bocked membrane Tension (T) plays a crucial role in lowering instability, demonstrating that the system's instability can be passively controlled by tuning these physical properties. The research revealed that the velocity slip at the wall has a disruptive effect at the onset of instability. These findings will contribute to a deeper understanding of flow stability in systems influenced by elastic surfaces and slippery boundaries.

REFERENCES

Anjalaiah, Usha R., and Séverine M. (2013). Thin film flow down a porous substrate in the presence of an insoluble surfactant: Stability analysis. *Physics of Fluids*, 25(2):022-101

Arka, D., Avinash K., and Chirodeep B. (2024). Interplay of fluid rheology and micro-patterning toward modulating draining characteristics on an inclined substrate. *Physics of Fluids*, 36(2).

Bhat, F. A. and Samanta A.(2018). Linear stability of a contaminated fluid flow down a slippery inclined plane. *Physical Review E*, 98(3):033-108.

Benney, D. J. (1966). Long waves on liquid films. *Journal of mathematics and physics*, 45(1-4):150–155.

Blyth, M. G. and Pozrikidis C. (2004). Effect of surfactant on the stability of film flow down an inclined plane. *Journal of Fluid Mechanics*, 521:241–250.

Camporeale, C., Canuto C., and Luca R. (2012). A spectral approach for the stability analysis of turbulent open-channel flows over granular beds. *Theoretical and Computational Fluid Dynamics* 26.1: 51-80.

Chang, H.H., Demekhin, E.A. (2002). Complex Wave Dynamics on Thin Films, *Elsevier, Amsterdam*.

Chicheng, M., Jianlin L., Shilin X., and Yongqi L. (2020). Contact line instability of gravity driven thin films flowing down an inclined plane with wall slippage. *Chemical Engineering Science*, 214:115-418.

Chin, R., Abernath, F., Bertschy, J. (1986). Gravity and shear wave stability of free surface flows. Part 1. numerical calculations. J. Fluid Mech. 168, 501–513.

Choudhury, A., and Samanta A. (2022). Linear stability of a falling film over a heated slippery plane. *Physical Review E*, 105(6):065-112.

Criminale, W.O., Thomas L., Jackson, and Ronald D. J. (2003). Theory and computation of hydrodynamic stability. *Cambridge University Press*.

Dholey, S. and Gorai S. (2021). Hydrodynamic instabilities of a viscous liquid film flowing down an inclined or vertical plane. *Physics of Fluids*, 33(10), 2021.

Ding, Z. and Wong, T. N. (2015). Falling liquid films on a slippery substrate with marangoni effects. *International Journal of Heat and Mass Transfer*, 90:689–701.

Kandel, H. N. and Pascal J.P. (2013). Inclined fluid-film flow with bottom filtration. *Physical Review E*, 88(5):052-405.

Karmakar, D. and Sahoo, T. (2008), Gravity wave interaction with floating membrane due to abrupt change in water depth. *Ocean Engineering*, 35(7):598–615.

Kao T. W. (1965), Role of the interface in the stability of stratified flow down an inclined plane. *The Physics of Fluids*, 8(12):2190–2194.

Kao T. W. (1968). Role of viscosity stratification in the stability of two-layer flow down an incline. *Journal of Fluid Mechanics*, 33(3):561–572.

Khan, M., Sani, M., Ghosh, S., & Behera, H. (2021). Poiseuille–Rayleigh–Bénard instability of a channel flow with uniform cross-flow and thermal slip. *Physics of Fluids*, *33*(5).

Li, C., Liu, C., Zhou, J., & Ye, X. (2023). Hydrodynamics and instabilities of a falling liquid film with an insoluble surfactant. *Physics of Fluids* 35(6).

Li, X., Pozrikidis, C. (1997). The effect of surfactants on drop deformation and on the rheology of dilute emulsions in stokes flow. J. Fluid Mech. 341, 165–194.

Liu, R. and Liu Q. (2009). Instabilities of a liquid film flowing down an inclined porous plane. *Physical Review E*, 80(3):036316.

Newman, J. N. (2018). Marine Hydrodynamics. *MIT press*.

O'Connor, J., and Benedict D. R. (2021). "A fluid–structure interaction model for free-surface flows and flexible structures using smoothed particle hydrodynamics on a GPU." *Journal of Fluids and Structures* 104: 103-312.

Oron, A., Davis, S. H., Bankoff, S. G. (1997). Long-scale evolution of thin liquid films. *Rev. Mod. Phys.* 69, 9-31.

Otis D. R. Jr, M. Johnson, Pedley, T. J., and Kamm R. D. (1993). Role of pulmonary surfactant in airway closure: a computational study. *Journal of Applied Physiology*, 75(3):1323–1333.

Pascal J. P. (1999). Linear stability of fluid flow down a porous inclined plane. *Journal of Physics D: Applied Physics*, 32(4):417.

Pascal J. P. (2006). Instability of power-law fluid flow down a porous incline. *Journal of non- Newtonian fluid mechanics*, 133(2-3):109–120.

Pascal J. P. and D'Alessio S. J. (2010), Instability in gravity-driven flow over uneven permeable sur- faces. *International journal of multiphase flow*, 36(6):449–459.

Samaha M. A. and Mohamed G. Hak (2021). Slippery surfaces: A decade of progress. *Physics of Fluids*, 33(7).

Samanta, A. (2014). Shear-imposed falling film. Journal of fluid mechanics, 753:131-149.

Samanta, A. (2025). Effect of soluble surfactant on thermocapillary instability in falling film. *Physical Review Fluids* 10.6: 064001.

Samanta, A. (2023). Modal analysis of a fluid flowing over a porous substrate." *Theoretical and Computational Fluid Dynamics* 37(2): 241-260.

Samanta, A., Christian R., and Benoit G., (2011). A falling film down a slippery inclined plane. *Journal of Fluid Mechanics*, 684:353–383.

Sani M., Behera H., and Ghosh S. (2018). Stability analysis of a film flow down an incline in the presence of a floating flexible membrane. *International Conference on Mathematical Modelling and Scientific Computation*. Singapore: Springer Singapore.

Sani M., Behera H., and Ghosh S. (2020). Stability analysis of a film flow down an incline in the presence of a floating flexible membrane. In *Mathematical Modelling and Scientific Computing with Applications: ICMMSC 2018, Indore, India, Springer July 19–21*, 253–263.

Sani, M., Selvan, S. A., Ghosh, S., and Behera, H. (2020). Effect of imposed shear on the dynamics of a contaminated two-layer film flow down a slippery incline. *Physics of Fluids,* 32(10).

Sani, M., Sukhendu G., and Behera H. (2021). Effect of a floating elastic membrane for stabilizing the film flow down a porous inclined plane. *ZAMM-Journal of Applied Mathematics and Mechanics/Zeitschrift für Angewandte Mathematik und Mechanik* 101(2): e201900246.

Subham P. and Samanta A. (2021). Linear stability of a contaminated shear-imposed vis- coelastic liquid flowing down an inclined plane. *Physics of Fluids*, 33(12).

Thiele U., Andrew J. A., and Mathis P. (2012). Thermodynamically consistent description of the hydrodynamics of free surfaces covered by insoluble surfactants of high concentration. *Physics of Fluids*, 24(10).

Tripathi D., Prauteeto R., Ajay Vikram S., Vimal K., and Swarn L. S. (2023). Durability of slippery liquid-infused surfaces: challenges and advances. *Coatings*, 13(6):10-95.

Usha R., Millet S., Ben H., and François R. (2011). Shear-thinning film on a porous sub- strate: stability analysis of a one-sided model. *Chemical engineering science*, 66(22):5614–5627.

Vallentine, H. R. (2013). *Applied Hydrodynamics Springer*.

Wang C.Y. (1984). Thin film flowing down a curved surface. *Zeitschrift für angewandte Mathematik und Physik ZAMP*, 35(4):532–544.

Yih, C. (1963). Stability of liquid flow down an inclined plane. *The physics of Fluids*, 6(3):3.